Temperature Fields Induced by Low Power Focused Ultrasound in Soft Tissues During Gene Therapy. Numerical Predictions and Experimental Results

Barbara GAMBIN, Tamara KUJAWSKA, Eleonora KRUGLENKO,
Andrzej MIZERA[1] , Andrzej NOWICKI

Institute of Fundamental Technological Research
Polish Academy of Sciences
Pawińskiego 5B, 02-106 Warszawa, Poland
e-mail: bgambin@ippt.gov.pl

The aim of this work is twofold. Firstly, to verify a theoretical model which is capable of predicting temperature fields appearing in soft tissues during their ultrasound treatment. Secondly, to analyze some aspects of the dynamics of Heat Shock Response induced by the heating process in the context of therapeutic treatment. The theoretical investigations and quantitive analysis of temperature increments at any field point versus time of heating process, depending on the heat source power, spatial distribution and duration as well as on the tissue thermal properties, has been carried out by Finite Element Method (FEM). The validation of the numerical model has been performed by comparison of the calculation results with the experimental data obtained by measuring *in vitro* of the 3D temperature increments induced in samples of the turkey and veal liver by the circular focused transducer with the diameter of 15 mm, focal length of 25 mm and resonance frequency of 2 MHz. Various ultrasonic regimes were considered. They were controlled by adjusting ultrasound power and exposure time. The heat shock proteins (HSP) and misfolded proteins (MFP) levels during the proposed cyclic sonification are presented.

Keywords: heat-responsive gene therapy, temperature field, low-power focused ultrasound, soft tissues, ultrasonic regime control, heat sources distribution, heat shock proteins.

---

[1] The Autor is a Ph.D. student at the Institute of Fundamental Technological Research, Warsaw, Poland and at the Åbo Akademi University & Turku Center for Computer Science, Turku, Finland.

1. Introduction

1.1. Motivation. Heat-responsive gene therapy

The heat shock response (HSR) is a highly evolutionarily conserved defense mechanism, allowing the cell to promptly react to elevated temperature and other forms of environmental, chemical or physical stress. Exposure to shock conditions leads to misfolding of proteins, which in turn accumulate and form aggregates with disastrous effect for the cell. However, damage to cells can initiate one of two opposite responses: either apoptosis, the process of programmed cell death which prevents inflammation in multicellular organisms, or heat shock response which enables recovery and survival of the cell. Thus, these two pathways and the interplay between them have the decisive influence on the biological consequences of the stress. The key part of the heat shock response is an abrupt upregulation of the heat shock proteins (HSPs) which prevent the accumulation and aggregation of misfolded proteins. Two groups of heat shock proteins can be distinguished. Some heat shock proteins are constitutively and ubiquitously expressed in all eukaryotic cells. These proteins are called heat-shock cognates and are involved in house-keeping roles, e.g. assist nascent proteins in the establishment of proper conformation, transport (shuttle) other proteins between different compartments inside the cell and participate in signal transduction. The second group contains those, the expression of which is induced by stress. They act as chaperones, i.e. help proteins to maintain their structural integrity or assist the damaged proteins in re-establishment of the functional structure. Moreover, some of them can act as negative regulators of the apoptotic cascade [4] or aid the apoptotic machinery through their chaperone functions, see [15] for the review of this issue. These two functions fulfilled by the heat shock proteins, i.e. protein chaperoning and modulation of survival and death-signalling pathways, make them an attractive therapeutic target, for example in the case of neurodegenerative diseases [2, 7, 11] or cancer. Furthermore, the heat-induced expression of HSP genes is itself a mechanism of particular interest as it enables the design of heat-responsive gene therapy vectors, cf. [17].

In this study we consider hyperthermia, procedure of raising the temperature above 37°C, as a treatment modality both on the tissue and cellular level. Theoretically, a properly tuned tempo-spatial temperature distribution in tissue would lead to a desired heat shock response in the cells and, in consequence, enhanced expression of heat shock proteins which are important from the therapeutic point of view. One of the most relevant problems which arise in this context is related to the question whether an effective and controlled application of hyperthermia in the considered type of tissue is practically feasible. At the same time it is also important to assure that the increased temperature does not stimulate the ion activity within the cells and that the temperature itself is kept within the therapeutic range, i.e. up to 45°C. Also the tissue area and time of exposure to

heating must be precisely defined in order to activate the finely tuned heat shock response.

1.2. Advantages of the focused ultrasound

In order to meet requirements mentioned above, ultrasonic technique may be applied, cf. [6, 8, 16]. Technical improvements of the focused ultrasound ensure the non-invasive and strictly controlled heating of the target tissue volumes. Ultrasonic regimes can be controlled by adjusting the ultrasound beam's intensity, frequency, pulse duration, duty-cycle and exposure time. The control of spatial temperature distribution is of essential importance for correlation between the level of temperature and the level of the gene expression. Furthermore, it is crucial to establish safe protocols for heat-responsive gene therapy in a clinic. Besides, optimization of hyperthermia efficiency requires a precise and non-invasive estimation of internal temperature distribution. While there are several research trends for ultrasonic temperature estimation, the precise equipments for this purpose are still not available in clinical practice, cf. [1, 3, 5].

## 2. Experiments and numerical model

2.1. Experiments

The experimental set-up used for measurements is shown in Fig. 1a.

The acoustic pressure tone bursts were generated at the surface of a circular focused piezoceramic (Ferroperm Pz26, Norwey) transducer with the 2 MHz resonance frequency, 15 mm diameter and 25 mm focal length. The transducer was air-backed, had not a quarter wavelength matching layer and was driven at its resonance frequency by tone bursts of various numbers of cycles (20, 50, 100, 500) with the same duty-factor equal to 0.2. The amplitude of tone bursts generated by the arbitrary function generator (Agilent 33250A, Colorado Springs, USA) was varied from 105 mV_{pp} to 314 mV_{pp} and amplified by the power amplifier (ENI 3100LA, Rochester, USA). Then the voltage applied to the transducer was varied from 31.6 V_{pp} to 90 V_{pp}, producing the acoustic power on the transducer surface varied from 0.8 W to 6 W depending on the requirements imposed by the application. The tone burst waveforms were recorded using the digital oscilloscope (Tektronix TDS3012B, Beaverton, USA). The transducer was positioned in a tank filled with temperature-controlled distilled water. The source pressures used were determined with the calibrated bilaminar PVDF membrane hydrophone (Sonora Medical Systems Inc. SN S5-153, preamplifier P-159, Longmont, CO, USA), having an effective diameter of the sensitive element of 0.414 mm as well as with the power balance (Ohmic Instruments UPMDT1E, Easton, USA). The source pressure measurements with the hydrophone were made at the distance of 5 mm from the transducer centre and gave the average pressures varied from 0.24 MPa

to 0.654 MPa. The agreement between the both source pressure determination methods was within 10%.
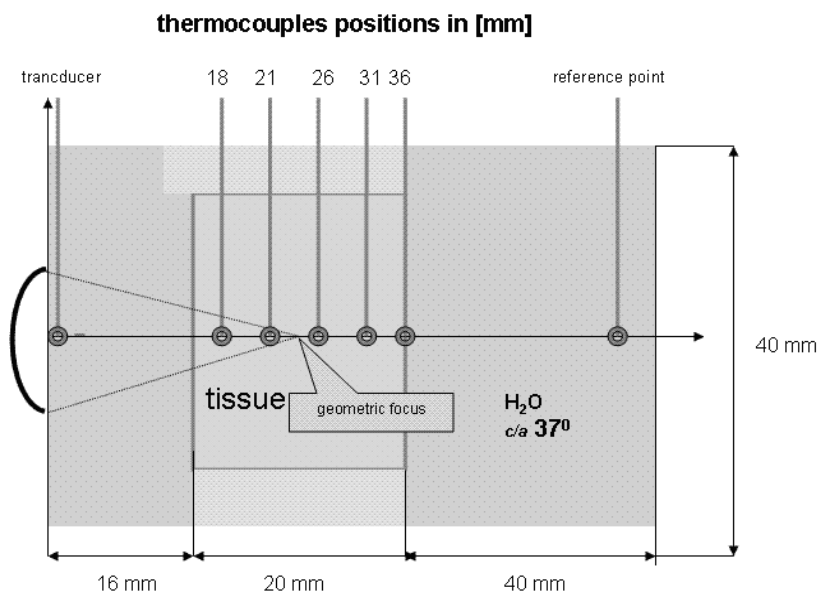
a)
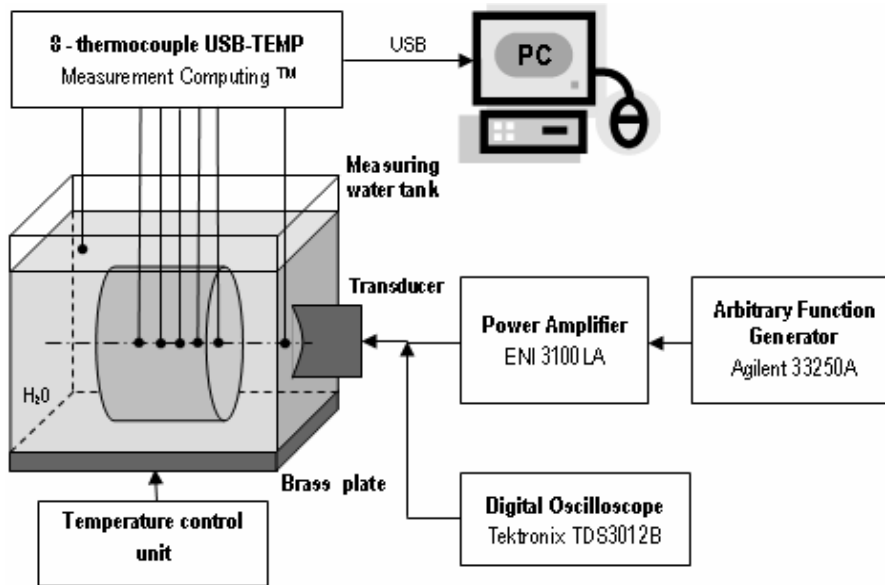
b)

Fig. 1. a) Block-diagram of the experimental set-up; b) Schematic illustration of experiment with marked positions of thermocouples.

The soft tissue being studied (turkey or veal liver) was placed in a cylindrical container with the 3 cm internal diameter and 2 cm height. The axis of both the container and transducer were overlapped. The container with the transparent for sound, 20 μm-thick polyethylene foil stretched over each end, was immersed in water tank. The distance between the transducer centre and the front foil plane of the sample was specific for the transducer chosen for measurements and equal to $z = 17$ mm. It was the distance at which sudden growth of the self-generated second and higher harmonics of the finite-amplitude wave generated from this transducer in water appears. The rectangular window at the top of the container was milled to enable the thermocouples to be inserted inside of the tissue sample. The thermocouples were introduced inside of the tissue through thin hypodermic needles fixed on the tank cover, in order to ensure the thermocouples parallelism and precise position along or across the acoustic beam axis.

The 8-thermocouples unit (USB-TEMP, Measurement Computing, Norton, USA) was used to detect the temperature induced by ultrasound in various field points along or across the acoustic axis. The measurements along the acoustic axis were carried out using seven thermocouples. Five of them were positioned along the acoustic axis at the distances from the transducer centre equal to $z = 18$ mm, 21 mm, 26 mm, 31 mm, 36 mm, respectively. The sixth thermocouple was located on the acoustic axis very close to the transducer radiating surface and the seventh one measured the reference temperature in the water tank which was controlled and stabilized using the temperature control unit. All measurements were performed at 37°C in temperature-controlled degassed distilled water. The temperatures measured versus exposure time were recorded by the USB-TEMP unit and transferred to the PC via USB slot. For processing and visualizing the data obtained the software program TracerDAQ was used.

Schematic illustration of the thermocouples positions geometry in relation to the transducer is shown in Fig. 1b.

In order to meet the requirements for thermal gene therapy applications, the temperature induced by the transducer in tissues in the focal area can not exceed 43°C. Preliminary measurements have shown that the temperature field in soft tissues considered does not depend on the tone burst duration but depends on the duty factor, average acoustic power on the transducer face and the exposure duration. The results of measurements have shown that in order to avoid the tissue heating over 43°C, the average acoustic power used for experiments should not be higher than 1 W. All experiments in this study have been done for the transducer acoustic power of 0.8 W.

The most important conclusion from Fig. 2 is a following: the maximal safe duration of irradiation has to be less than 2.5 min. For irradiation by a continuous wave, the temperature increases up to 43°C in the neighborhood of the position of the physical focus (21 mm) of the transducer. Then, the defense mechanism of the HSR does no longer protect against protein denaturation.
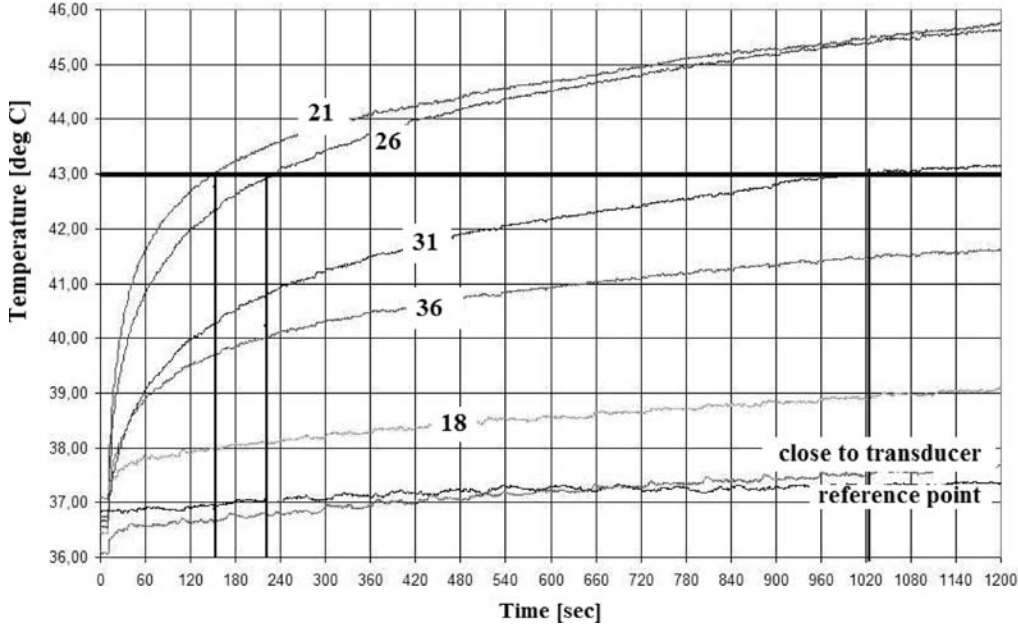
Fig. 2. Temperature variation in time measured by thermocouples along the acoustic axis at various distances from transducer.

2.2. Description of the model

Bioheat transfer equation in an inhomogeneous thermally anisotropic medium, occupying domain V in the 3D real space, may be written as:

$$\rho(\mathbf{x})C(\mathbf{x})\frac{\partial T(\mathbf{x},t)}{\partial t} = \nabla \cdot K(\mathbf{x}) \cdot \nabla T(\mathbf{x},t) + Q_p(\mathbf{x},t)$$
$$+ Q_{\text{int}}(\mathbf{x},t) + Q_{\text{ext}}(\mathbf{x},t), \qquad \text{for} \qquad \mathbf{x} \in V, \qquad (1)$$

where T, t, ∇, ρ, K, Q_p, Q_{int}, Q_{ext} denotes temperature, time variable, gradient vector, density, specific heat, thermal conductivity of a medium, in the case of 2nd order tensor, perfusion, internal heat generation and external heating, e.g. by irradiation processes, respectively, see [12]. The bioheat equations in many different forms are given in literature, see e.g. [18] . On the basis of the experiment described above, the initial boundary value problem of the bioheat Eq. (1) can be stated. It is evident that for the tissue, *in vitro* perfusion and internal heat generation disappear, so equalities

$$Q_p(\mathbf{x},t) = 0, \qquad Q_{\text{int}}(\mathbf{x},t) = 0 \qquad (2)$$

are substituted in Eq. (1). The medium under consideration consists of two materials occupying the domain $V = V_w \cup V_t$, V_w – water and V_t – tissue, respectively, cf. Fig. 3.
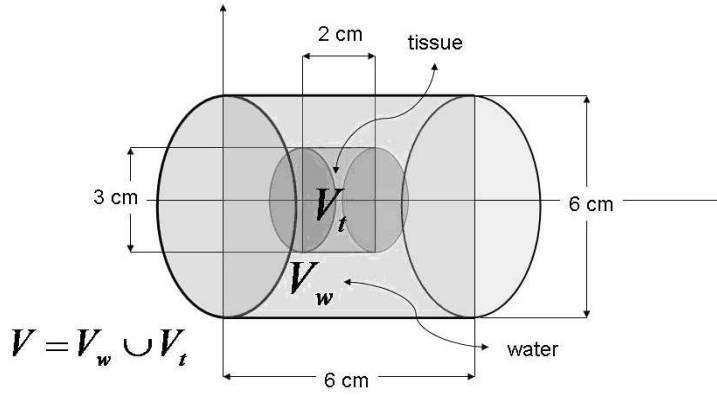
Fig. 3. Two domains occupied by water and tissue used in numerical calculations.

The properties of two homogeneous and isotropic materials are listed below in Table 1.

Table 1. Material properties of water and tissue used in numerical calculations.

Material	Water	Soft tissue
Density [kg/m^3]	$\rho_w = 1000$	$\rho_t = 1060$
Specific heat [J/(kg K)]	$C_w = 4200$	$C_t = 3800$
Conductivity [W/(m K)]	$K_w = 0.6$	$K_t = 0.5$

Then, in Eq. (1) the coefficients take the form

$$\rho(\mathbf{x}) = \begin{cases} \rho_w & \text{for} \quad \mathbf{x} \in V_w \\ \rho_t & \text{for} \quad \mathbf{x} \in V_t \end{cases},$$

$$C(\mathbf{x}) = \begin{cases} C_w & \text{for} \quad \mathbf{x} \in V_w \\ C_t & \text{for} \quad \mathbf{x} \in V_t \end{cases}, \tag{3}$$

$$K(\mathbf{x}) = K\mathbf{I},$$

$$K = \begin{cases} K_w & \text{for} \quad \mathbf{x} \in V_w \\ K_t & \text{for} \quad \mathbf{x} \in V_t \end{cases}, \quad \text{for} \quad \mathbf{x} \in V,$$

where $\mathbf{I}$ denotes unit second order tensor.

The temperature on the boundary ∂V of the domain V is assumed to be constant, namely

$$T(\mathbf{x}, t) = 37°\text{C}, \qquad \mathbf{x} \in \partial V. \tag{4}$$

The external heat Q_{ext} is modeled by uniformly distributed heat sources of the fixed power, namely 0.16 W and 0.8 W, in the domain depicted in Fig. 4.
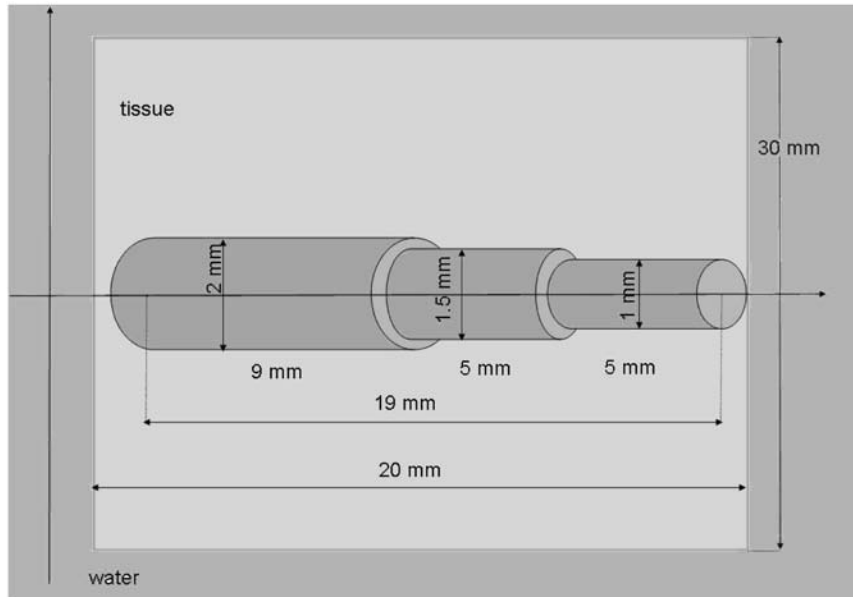
Fig. 4. The heat sources form assumed in numerical calculations.

The heat sources are assumed to be produced by the focused acoustic beam inside the tissue and their geometrical distribution are chosen in a way to minimize, as far as possible, the difference between numerical results and experimental data. The Eqs. (1)–(4) together with fixed heat sources distribution (in the performed calculations the distribution depicted on Fig. 4 was used) provide the well-defined boundary-value problem for the Pennes Eq. (1). The solution is obtained numerically with using the standard Finite Element Method (FEM).

3. Results

The Abaqus 6.9 software (DS Simulia Corp.) was used to solve the problem formulated above. The numerical calculation results were fitted to the experimental data by adjusting the input parameters of the numerical model: the shape and power of the heat sources. The calculated temperature increase along the beam axis is depicted in Fig. 5. and the numerical values in the points of thermocouples locations together with measurements are given in Table 2. The rate of temperature rise predicted by the model is overestimated with respect to the measured one. In accordance with the numerical simulation, the safe time of irradiation is less than 1 min. The reason for that is the assumed shape of heat sources distribution, which is unrealistic and it is considered only as a first approximation. More realistic, continuous distribution of heat sources directly connected with the acoustic field converted into heat should be studied.
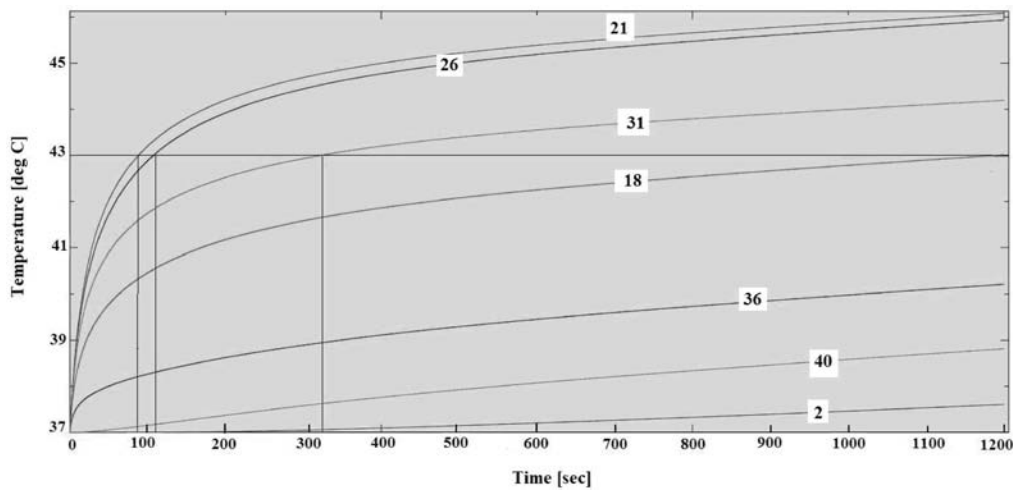
Fig. 5. Temperature variation in time predicted by numerical calculations.

Table 2. Comparison of the temperature elevation measured by the thermocouples in the chosen points with the numerical calculation results.

Axial distance from transducer in [mm]	18	21	26	31	36
Measured temperature increment in [°C]	2.1	8.76	8.64	6.1	4.65
Numerical results – heat sources power 0.16 [W]	2.8–1.8	7.6–8.3	7.8–8.1	3.6–4.0	1.0–1.2
Numerical results – heat sources power 0.2 [W]	6.7–7.2	8.5–9.0	8.1–8.6	5.4–5.9	2.2–2.7

Illustrations of the tissue heating patterns (along and across the beam axis) are shown in Fig. 6 and Fig. 7. The temperature elevation profiles versus axial and radial distances from the transducer are shown in Fig. 8. The temperature elevation profiles as well as the temperature pattern in the tissue, were obtained recently by the authors of presentation [9] without using the MES calculations and with using solutions to a different boundary value problem. However, there are qualitative similarities between the results.

Preliminary sensitivity analysis of the temperature distribution with respect to the boundary conditions and, independently, to material properties values, leads to the following conclusions. If the temperature is fixed on the boundary of the water tank, the temperature elevation is several degrees higher than in the case of the boundary condition stated in (4). It suggests that the process of heat transfer in the water is mainly due to the convection phenomena rather than to the conductivity assumed in our model. The change of specific heat of tissue by 10% implies changes of temperature increment of several per mille,
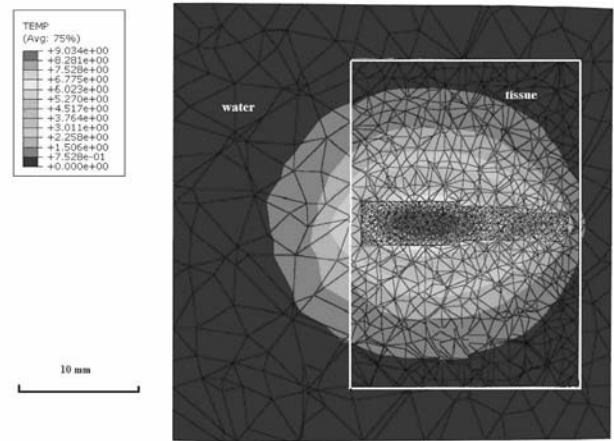
Fig. 6. Temperature pattern in the tissue along the acoustic beam axis.
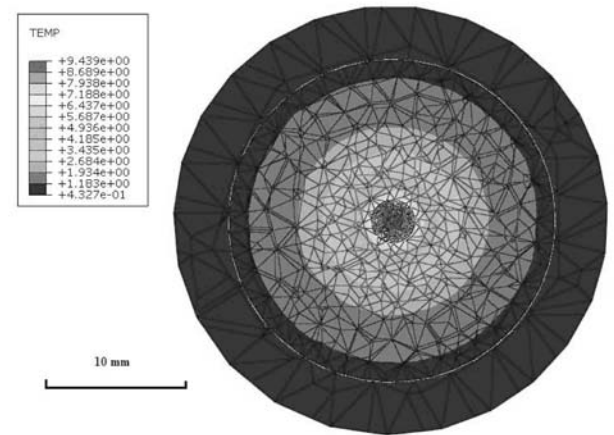

Fig. 7. Temperature pattern in the tissue across the acoustic beam axis at the axial distance 26 mm from the transducer.
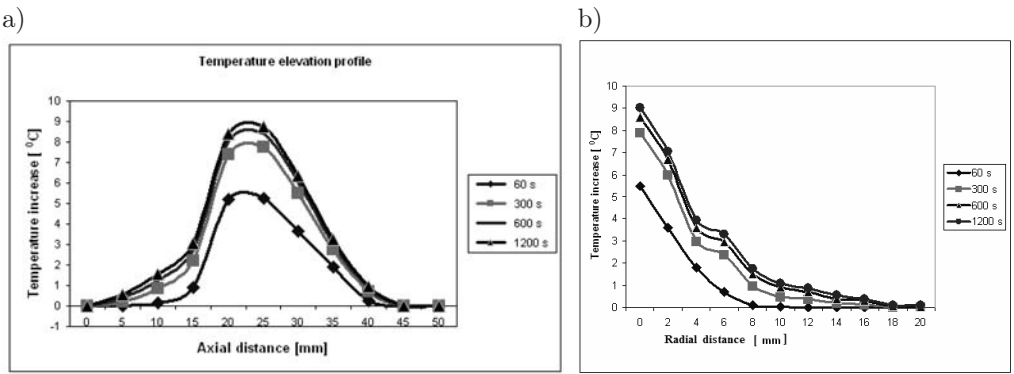
a)

b)

Fig. 8. Temperature elevation profiles versus axial and radial distance from the transducer.

cf. Table 3. In contrast, a change in tissue thermal conductivity by 10% implies a proportionate increase in temperature, compare Table 4. It means that in the model one can control the level of temperature increment not only by changes of heat sources but also by changing the conductivity coefficient. The problem how to define properly the conductivity coefficient of soft tissue is still open, cf. [19]. The assumed in calculations material properties may significantly differ from the properties of tissue used in the experiment. This asks for a more thorough sensitivity analysis.

Table 3. Sensitivity of temperature rise for various specific heat of tissue.

Axial distance from transducer in [mm]	18	21	26	31	36
Specific heat 3800 in [J/kg K]	6.86	8.82	8.46	5.45	2.36
Specific heat 3520 in [J/kg K] (change in %)	6.88 (0.29%)	8.84 (0.23%)	8.48 (0.24%)	5.46 (0.18%)	2.37 (0.42%)
Specific heat 4180 in [J/kg K]	6.84	8.80	8.44	5.42	2.36

Table 4. Sensitivity of temperature rise for various conductivity of tissue.

Axial distance from transducer in [mm]	18	21	26	31	36
Conductivity 0.5 in [W/mK]	6.86	8.82	8.46	5.45	2.36
Conductivity 0.45 in [W/mK] (change in %)	7.46 (8.7%)	9.69 (9,8%)	9.32 (10,1%)	5.99 (9,9%)	2.56 (8,4%)
Conductivity 0.55 in [W/mK]	6.36	8.11	7.75	5.00	2.21

4. Dynamics of HSR

In order to utilize hyperthermia for therapeutic purposes, a tissue heating scheme which would satisfy certain conditions needs to be designed. The most basic requirements are the following. First, the temperature at any place at any time of the heating process should not exceed 45°C. Second, the level of HSP should be higher than the level of HSP under physiological conditions, i.e. at the temperature of 37°C. At the same time, the level of the misfolded proteins (MFP) should be kept as low as possible due to the damaging effects it has on cell functioning.

In this presentation we propose a heating scheme which meets these requirements. It was obtained by performing numerical simulations of the model discussed in Subsec. 2.2. The temperature at the focal point was considered. First, the heat sources were turned on at the initial temperature of 37°C. The heating was turned off when the temperature reached 45°C. The cooling process was interrupted by turning on the heating again when the temperature decreased to 38°C. The last two phases, i.e. cooling and heating, where repeated periodically 26 times and the temperature time-course profile depicted in Fig. 9 was obtained. In Fig. 10 the temperature changes at different distances from the transducer in the first cycle are depicted. Further, the heating scheme was validated by performing numerical simulations of the basic heat shock response model presented
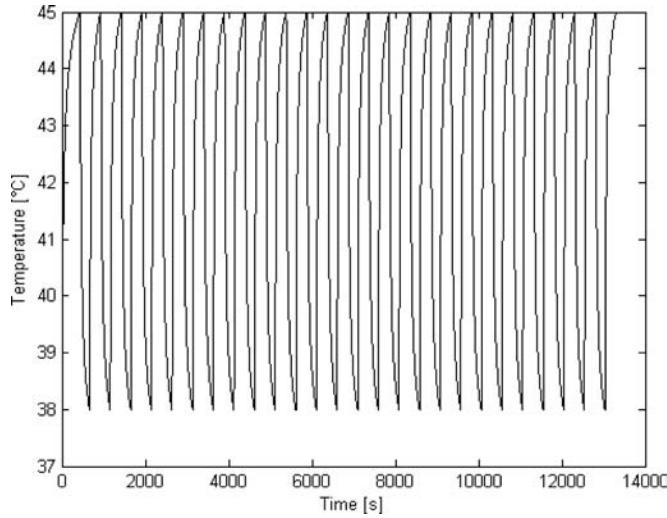

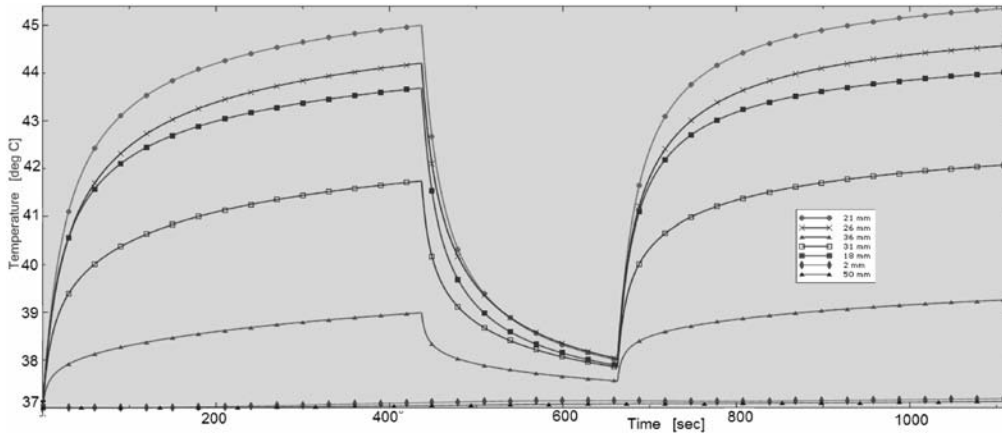Fig. 9. Temperature profile at the focal point (26 cycles of sonification).

Fig. 10. Temperature profile at different distances from the transducer (the first 1200 second of sonification).
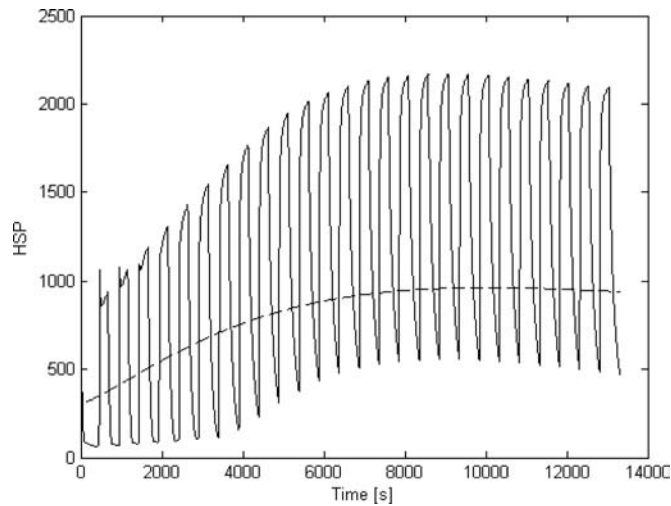
Fig. 11. HSP level caused by the applied cyclic heating scheme and the HSP level (dashed line) in reaction to constant temperature value ($42°$C).
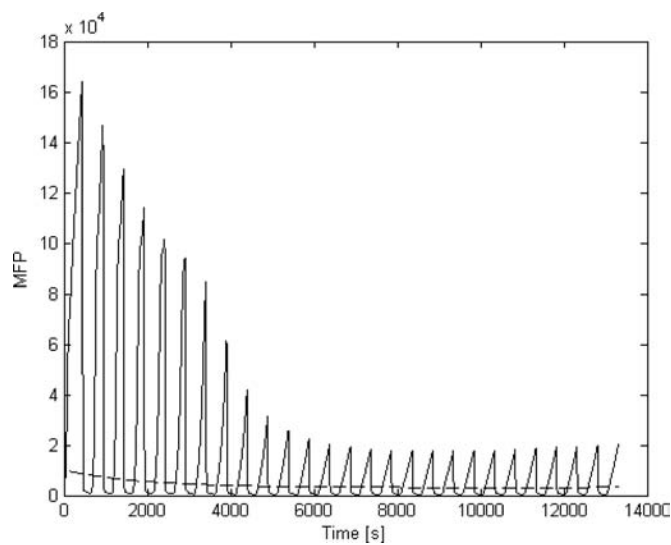

Fig. 12. MFP level caused by the applied cyclic heating scheme and the MFP level (dashed line) in reaction to constant temperature value ($43°$C).

recently in [13, 14]. Instead of a fixed temperature value, the obtained profile was used. The resulting behavior of the basic HSR model is shown in Figs. 11 and 12.

From the above results it is evident that the HSR caused by the cyclic soni-fication leads to the mean level of HSP not lower than in the reaction to a fixed temperature. At the same time the average MFP level shows a tendency toward decrease. Hence, the requirements stated above are met.

5. Concluding remarks

Based on the results of the performed experiment (Subsec. 2.1), for the physical process of the soft tissue heating by the focused ultrasound, the mathematical model of the linear heat transport has been formulated (Subsec. 2.2). Numerical solutions to this problem are given together with a preliminary sensitivity analysis (Sec. 3). The obtained results are used to illustrate the dynamics of HSR (Sec. 4) based on the recently elaborated model of HSR by the fourth author of this work ([10, 13, 14]). Furthermore, a cyclic sonification fulfilling certain therapeutic requirements is proposed.

In the blood supplied tissue, the perfusion itself could possibly stabilize the temperature level, but this has not been experimentally proved *in vitro* in the case of the focused ultrasound heating. However, in cases where the perfusion is inefficient or the heating tissue area is thermally isolated (fatty tissue), the model results presented in Sec. 4 may contribute to the planning of thermally induced gene therapy. Unfortunately, biological experiments which would confirm the presented results are still missing.

Additionally, the main objective of further engineering research is the construction of an integrated ultrasound device, which could be used not only for controlled heating in the desired tissue, but also for temperature determination (as an "acoustic thermometer").

Acknowledgments

References

[1] Arthur R.M., Straube W.L., Trobauch J.W., Moros E.G., *Non-invasive estimation of hyperthermia temperatures with ultrasound*, Int. J. Hyperthermia, **21**, 6, 589–600, September 2005.

[2] Balch W.E., Morimoto R.I., Dillin A., Kelly J.W., *Adapting proteostasis for disease intervention*, Science, **319**, 916–919 (2008).

[3] Bazan I., Vazques M., Ramoz A., Vera A., Leija L., *A performance analysis of echographic ultrasonic techniques for non-invasive temperature estimation in hyperthermia range using phantoms with scatterers*, Ultrasonics, **49**, 49358–376 (2009).

[4] Beere H.M., *The stress of dying: the role of heat shock proteins in the regulation of apoptosis*, J. Cell Sci., **117**, 13, 2641–2651 (2004).

[5] Daniels M.J., Jiang J., Varghese T., *Ultrasound simulation of real-time temperature estimation during radiofrequency ablation using finite element models*, Ultrasonics, **48**, 40–55 (2008).

[6] Humphrey V.F., *Ultrasound and matter – Physical interactions*, Progress in Biophysics and Molecular Biology, **93**, 195–211 (2007).

[7] Kalmar B., Kieran D., Greensmith L., *Molecular chaperones as therapeutic targets in amyotrophic lateral sclerosis*, Biochemical Society Transactions, **33**, 551–552 (2005).

[8] Kujawska T., Wójcik J., Filipczyński L., *Possibile temperature effects computed for acoustic microscopy used for living cells*, Ultrasound in Med. & Biol., **30**, 1, 99–101 (2004).

[9] Kujawska T., Wójcik J., Nowicki A., *Temperature Fields in Soft Tissue during LPUS Treatment: Numerical Prediction and Experiment Results*, will appear in: Proceedings of the 9th International Symposium on Therapeutic Ultrasound, 23–26 September 2009, Aix en Provence, France.

[10] Mizera A., Gambin B., *Stochastic modelling of the eukaryotic heat shock response*, submitted for publication, 2009.

[11] Morimoto R., *Proteotoxic stress and inducible chaperone networks in neurodegenerative disease and aging*, Genes Dev., **22**, 1427–1438 (2008).

[12] Pennes H.H., *Analysis of tissue and arterial blood temperatures in the resting human forearm*, J. Appl. Physiol., **1**, 93–122 (1948).

[13] Petre I., Mizera A., Back R.J., *Computational heuristics for simplifying a biological model*, [in:] *Mathematical Theory and Computational Practice*, Ambos-Spies K., Löwe B., Merkle W. [Eds.], Vol. 5635 of Lecture Notes in Computer Science, Springer, 2009.

[14] Petre I., Mizera A., Hayder C.L., Mikhailov A., Eroksson J.E., Sistonen L., Back R.J., *A new mathematical model for the heat shock response*, [in:] *Algorithmic bioprocesses*, Natural Computing, Kok J. [Ed.], Springer, 2008.

[15] Takayama S., Reed John C., Homma S., *Heat-shock proteins as regulators of apoptosis*, Oncogene, **22**, 9041–9047 (2003).

[16] Ter Haar G.R., *The Resurgense of Therapeutic Ultrasound – A 21st Centurey Phenomenon*, Ultrasonics, **48**, 233 (2008).

[17] Walther W., Stein U., *Heat-responsive gene expression for gene therapy*, Advanced Drug Deliery Reviews, **61**, 641–649 (2009).

[18] Weinbaum S., Jiji L., *A new simplified bioheat equation for the effect of the local blood flow on local average tissue temperature*, J. Biomech. Eng., 131–139 (1985).

[19] Yuan Ping, *Numerical analysis of an equivalent heat transfer coefficient in a porous model for simulating a biological tissue in a hyperthermia therapy*, International Journal of Heat and Mass Transfer, **52**, 7–8, 1734–1740 (2009).